Effect of Pedestrian Movement on MIMO-OFDM Channel Capacity in an Indoor Environment

Jishu Das Gupta, *Student Member, IEEE,* Hajime Suzuki, *Member, IEEE* and Karla Ziri-Castro, *Member, IEEE*

***Abstract*—Effects of pedestrian movement on multiple-input multiple-output orthogonal frequency division multiplexing (MIMO-OFDM) channel capacity have been investigated using experiment and simulation. The experiment was conducted at 5.2 GHz by a MIMO-OFDM packet transmission demonstrator using four transmitters and four receivers built in-house. Geometric optics based ray tracing technique was used to simulate the experimental scenarios. Changes in the channel capacity dynamic range have been analysed for different number of pedestrian (0-3) and antennas (2-4). Measurement and simulation results show that the dynamic range increases with the number of pedestrian and the number of antennas on the transmitter and receiver array.**

***Index Terms*—MIMO systems, propagation measurements, temporal variation.**

I. Introduction

MULTIPLE-INPUT MULTIPLE-OUTPUT orthogonal frequency division multiplexing (MIMO-OFDM) is currently being considered as a strong candidate for the physical layer transmission scheme of next generation broadband wireless communication systems [1, 2]. In recent years, there has been an increase in the study of MIMO-OFDM channels in indoor environments [3, 4]. In indoor environments, the movement of personnel, industrial machinery, vehicles and various equipment can introduce temporal channel variations, which cause temporal fluctuation of MIMO-OFDM channel performance. The effects have been studied for narrow-band single carrier MIMO channels in [5] considering human body shadowing. However, only a few studies have been reported for MIMO-OFDM channels. In order to accurately assess the effects of human movement on MIMO-OFDM channels, it is important to consider frequency correlation, which cannot be obtained from the analysis of single carrier MIMO channels. Previously, the authors reported on the measured correlation, capacity, and dynamic range of the MIMO-OFDM for temporally varying channels [6–8].

This paper investigates the measured and simulated effects of human body movement on MIMO-OFDM channels within an indoor environment. The experiment was conducted using a MIMO-OFDM packet transmission demonstrator with four transmitters and four receivers, denoted 4×4. Geometric optics based ray tracing technique [9] was used to simulate the experimental scenarios, including pedestrians.

The remaining of this paper is organized as follows: Section II describes the criteria used to calculate the MIMO-OFDM capacity. Details on the measurements and simulations are given in Section III. Results are given in Section IV, followed by the conclusions in Section V.

II. MIMO-OFDM channel capacity

The MIMO-OFDM channel capacity without the knowledge of the channel at the transmitter is given by [4]

$$\bar{C} = \frac{1}{n_f}\sum_{k=1}^{n_f}\sum_{j=1}^{n_t}\log_2(1+\frac{\rho\gamma_j(f_k)}{n_t}), \quad (1)$$

where $\bar{C}$ is the normalized capacity in bits/sec/Hz, n_f is the number of OFDM sub-carriers, n_t is the number of Tx antennas, ρ is the average signal to noise ratio (SNR) and γ_j is the eigenvalue of $\mathbf{H}(f_k)\mathbf{H}(f_k)^H$. $\mathbf{H}(f_k)$ is the normalized channel coefficient matrix at sub-carrier f_k and $(.)^H$ denotes Hermitian transpose. The normalization is performed such that [10]

$$\mathrm{E}\left(||\mathbf{H}||_F^2\right) = n_t n_r, \quad (2)$$

where $\mathrm{E}(\cdot)$ denotes the expected value, $||\cdot||_F$ denotes the Frobenius norm, and n_r is the number of Rx antennas.

Two different criteria are employed to evaluate the MIMO-OFDM channel capacity. The first assumes an interference-limited system where transmitting power can be adjusted without a limit to provide a fixed average SNR at the receivers. The averaging of SNR and normalization of channel coefficient matrix is performed over all MIMO sub-channels and over all OFDM sub-carriers. This criterion is called fixed SNR capacity. It corresponds to the system where co-channel interference is the limiting factor for the system capacity, and enough Tx power is reserved to cater for every location within the coverage area. SNR=15 dB is used in the following analysis.

The second criterion assumes a power-limited system where the transmitting power is fixed. In this case the averaging of SNR and normalization of channel coefficient matrix is performed over all MIMO sub-channels, OFDM sub-carriers, measurement samples, and different number of pedestrian. This is called fixed Tx power capacity. It incorporates the effects of the reduction of power due to body shadowing by the pedestrian. This criterion is more suitable for the analysis of WLAN system where the transmitting power is typically fixed.

Manuscript received December 22, 2008; revised February 12, 2009 and May 1, 2009.

J. Das Gupta and K. Ziri-Castro are with the Faculty of Built Environment and Engineering, School of Engineering Systems, Queensland University of Technology, Australia, (e-mail: j.dasgupta@qut.edu.au).

H. Suzuki is with the ICT Centre, Commonwealth Scientific and Industrial Research Organisation (CSIRO), PO Box 76, Epping, NSW 1710 Australia (e-mail: Hajime.Suzuki@csiro.au).

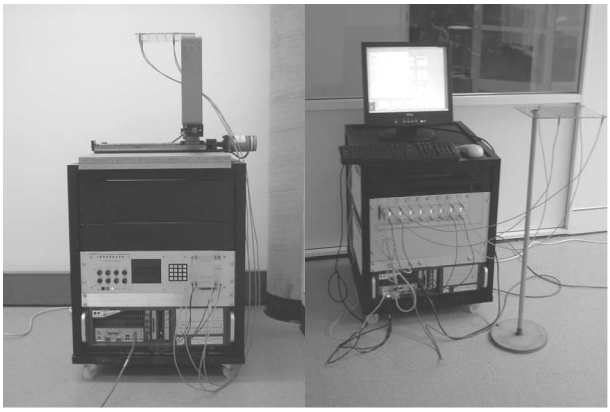

Fig. 1. MIMO-OFDM demonstrator from CSIRO ICT Center (left: Tx, right Rx).

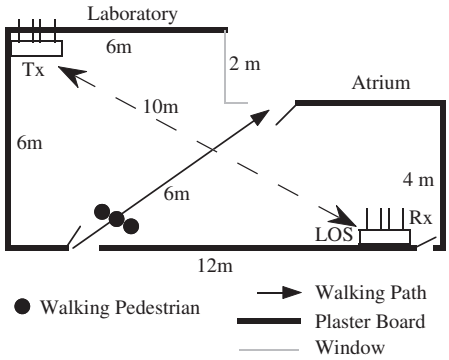

Fig. 2. Experiment floor plan.

III. Description of Measurements and Simulations

A. Measurement details

Actual MIMO-OFDM channel coefficients were measured by the MIMO-OFDM packet transmission demonstrator developed by CSIRO ICT Centre [11]. The demonstrator operates at a carrier frequency of 5.24 GHz with the bandwidth of 40 MHz. The OFDM sub-carrier spacing and operational bandwidth closely follow those of the IEEE 802.11n draft standard [12]. The dynamic range of the demonstrator was better than 40 dB. The demonstrator is shown in Fig. 1. Further technical specifications for the demonstrator can be found in [11, 13].

Identical off-the-shelf omnidirectional loop antennas (Sky-Cross SMA-5250-UA) are used as both Tx and Rx antenna array elements. The four antenna elements are arranged to form a uniform square array on the horizontal plane. The spacing of the antenna elements is set to 3 wavelengths at Tx and 2 wavelengths at Rx. The antenna spacing is considered to be large enough [4] so that the exact value of the antenna spacing does not affect the MIMO-OFDM channel capacity.

Measurements were performed on the furniture free ground floor room in the CSIRO ICT Centre, Marshfield, Sydney as shown in Fig. 2. Both Tx and Rx, separated by 10 m, are located inside the same 57 m^2 laboratory. During one measurement scenario, 1 to 3 pedestrians walked together along a 6 m trajectory. Complex channel coefficients for each of 16 MIMO sub-channels at 114 OFDM sub-carriers were collected at 100 time samples while pedestrians were walking. Due to the hardware limitation, the sampling rate of the measurement was limited to approximately 2 samples/sec, and hence pedestrian moved slower than usual (less than 1 km/hour). We note that the capacity dynamic range, as defined in Section IV, does not depend on the speed of the pedestrian or on the sampling rate as long as enough measurement points are collected. The measurements were performed once for each scenario.

B. Simulation Details

The frustum ray tracing technique [9] was used to simulate the measurement scenarios. This technique has the advantage of accurately modeling radio propagation (specular reflection) in a three dimensional environment efficiently. For the simulations, walls are modeled as single slabs whose permittivity and permeability are determined from penetration loss measurement of the actual material [14]. In previous studies using the frustum ray tracing algorithms, [9], it was found that with a maximum of 4 reflections, accurate channel prediction was achieved in an indoor line-of-sight (LoS) environment. Hence we have opted to use up to 4 consecutive reflections for the simulated scenarios. The algorithms were implemented on MATLAB with double-precision floating-point values. The OFDM parameters used in the simulations are identical as those used for the measurements. The aim of the simulation is to capture the variation trend of the capacity dynamic range, rather than predicting the exact MIMO-OFDM channel at the time of the measurement. A very simple model of the human body was employed (a rectangular block with a dimension of 0.62 m depth, 0.31 m width and 1.70 m height with the permittivity and conductivity characteristics of a real human body [5]). Diffraction and scattering were not included in the analysis. One simulation was performed for different receiver antenna array locations defined on a grid within an area of two wavelengths times two wavelengths with 0.1 wavelength resolution resulting in 400 locations, in order to observe the variation of the capacity dynamic range as a function of small scale displacement of the antennas. While small variation in the capacity dynamic range was observed depending on the exact location of the receiver antenna array, the dynamic range results are averaged over 400 receiver antenna array locations to obtain the trend as a function of the number of antennas and of pedestrian.

IV. Results

Fig. 3 shows an example temporal variation of the measured fixed SNR 4×4 MIMO-OFDM channel capacity when one pedestrian is crossing. It can be seen that the capacity increased as a personnel crossed the direct LoS path. In [5], capacity dynamic range had been defined as the difference between the maximum and the minimum value of the MIMO channel capacity. In this paper, we define 90% capacity dynamic range which is the difference between the top 95% and the bottom 5% values, in order to remove extreme cases. 90% capacity dynamic range can also be defined from the

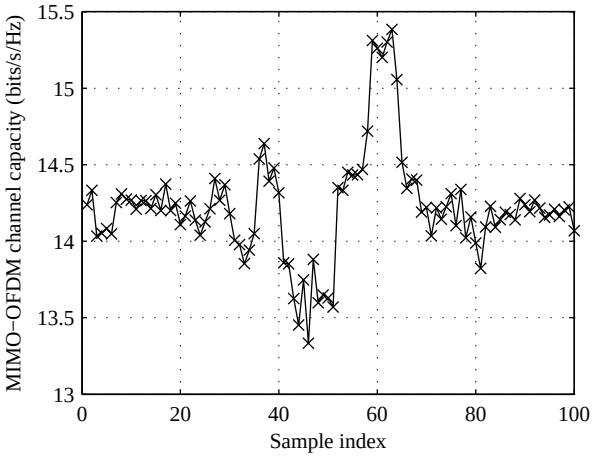

Fig. 3. Example measured temporal variation of 4×4 MIMO-OFDM fixed SNR channel capacity with 1 pedestrian (2 samples per second).

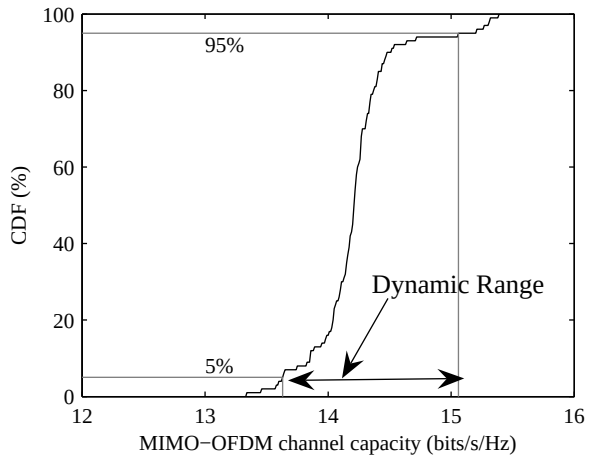

Fig. 4. Example measured CDF of 4×4 MIMO-OFDM fixed SNR channel capacity with 1 pedestrian.

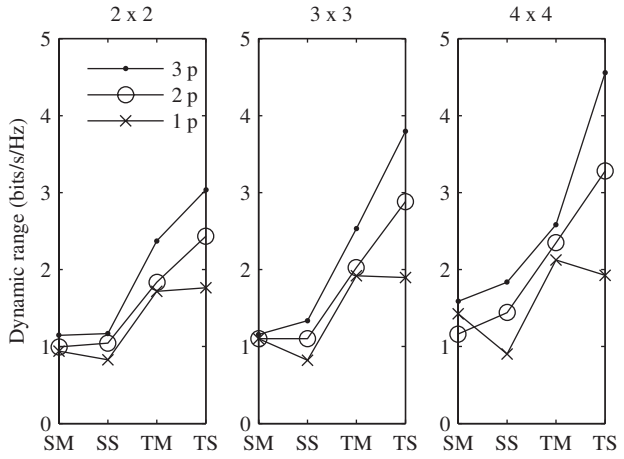

Fig. 5. Dynamic range variation with different number of pedestrian and antennas. SM: fixed SNR, measurement. SS: fixed SNR, simulation. TM: fixed Tx power, measurement. TS: fixed Tx power, simulation.

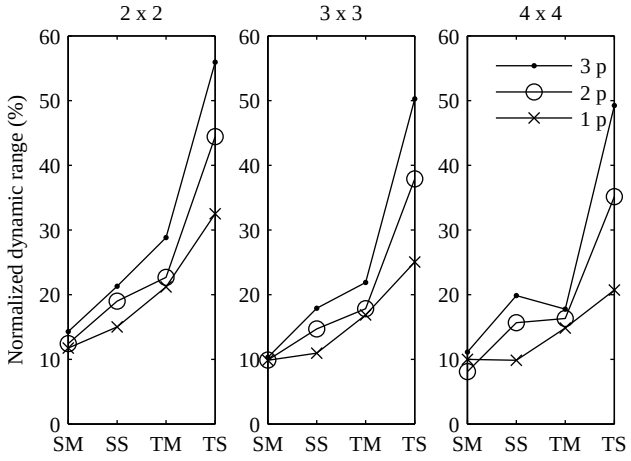

Fig. 6. Percentage dynamic range variation with different number of pedestrian and antennas. SM: fixed SNR, measurement. SS: fixed SNR, simulation. TM: fixed Tx power, measurement. TS: fixed Tx power, simulation.

cumulative distribution function (CDF) of the MIMO-OFDM channel capacity as shown in Fig. 4, which corresponds to the results presented in Fig. 3. The measured 4×4 fixed SNR capacity dynamic range without pedestrians was 0.16 bits/s/Hz. The main cause of this slight variation in channel capacity is considered to be due to disturbances outside the room at the time of measurements.

MIMO-OFDM channels corresponding to 2×2 and 3×3 are extracted from 4×4 results both for the measurement and simulation using all possible antenna combinations. Note that the results include different antenna spacing by using adjacent or diagonal antenna elements. Since the antenna spacing is large, the exact antenna spacing is considered to have small effects on the results. The dynamic range results for 2×2 and 3×3 are averaged over different combinations to provide representative values.

Fig. 5 shows the variation in the capacity dynamic range as a function of the number of pedestrian and antennas for fixed SNR or fixed TX power capacity by measurement and simulation. In general, we observe that the measured and simulated 90% capacity dynamic range is larger for the fixed Tx power criterion than for the fixed SNR. This is because the reduction in channel capacity values due to human-body shadowing effects is much more noticeable than the expected increase in capacity due to the de-correlation of the channel caused by the obstruction of the direct LoS path for the fixed Tx power criteria. From Fig. 5, we observe that the trend of capacity dynamic range increasing with the number of pedestrians is captured both by the measured and simulated results. With an increased number of pedestrians, a larger reduction of the LoS power is introduced, and hence a larger dynamic range results for the fixed Tx power capacity. For the fixed SNR capacity, the blocking of the LoS path by a larger number of pedestrian introduces a further de-correlation of the channel, and hence the fixed SNR capacity dynamic range also increases with the number of pedestrian. This has been confirmed by the measurements and the simulations for 0 to 3 pedestrians.

We also observe that both measurements and simulations

show that the capacity dynamic range slightly increases with the number of antenna used. The increase of the dynamic range as a function of the number of antennas is considered to be due to the increase in the MIMO-OFDM capacity with the number of antennas. To verify this point, the normalized dynamic range, which is the ratio of the dynamic range value with respect to the median capacity, is plotted in Fig. 6. While the trend of increasing dynamic range with the number of pedestrian is held, the relationship between the normalized dynamic range and the number of antennas is reversed. Here we observe that, when the dynamic range is scaled by the median capacity, a larger number of antennas tend to provide a smaller variation in the normalized dynamic range. This is considered to be due to increased path diversity by a larger number of MIMO channels with the larger number of antennas. While it may be desired to obtain more stable (less absolute dynamic range) MIMO-OFDM channel performance with increase in the number of antennas, both measurements and simulations show that the absolute capacity dynamic range slightly increases with the number of antenna used. The system designer needs to consider how one might mitigate the absolute dynamic range to provide stable performance in the presence of moving objects with increasing number of antennas.

We note that a large deviation of the simulation results from the measured results is observed for fixed Tx power criterion. This is considered to be due to the simplicity of the models of moving human-bodies and of the environment employed in the simulations.

V. Conclusion

We have observed that the MIMO-OFDM channel capacity dynamic range increases with the number of pedestrian, with 0 to 3 pedestrians, and with the number of antennas at the transmitter and receiver arrays, from 2 to 4 antennas in an indoor environment. Future effort should be directed to the analysis of different types of environments and pedestrian movements such as, meeting rooms and cafeterias where MIMO-OFDM based wireless communication systems are increasingly being used.

Acknowledgment

The authors would like to acknowledge the CSIRO ICT Centre personnel at Marshfield, Sydney, for providing the MIMO-OFDM packet transmission demonstrator and measurement sites. The authors also wish to thank anonymous reviewers for their valuable comments.

References

[1] C. Dubuc, D. Starks, T. Creasy, and Y. Hou, "A MIMO-OFDM prototype for next-generation wireless WANs," *IEEE Communications Magazine*, vol. 42, pp. 82–87, Dec 2004.

[2] W. Zhang, X. Xiang-Gen, and K. B. Letaief, "Space-time-frequency coding for MIMO-OFDM in next generation broadband wireless systems," *IEEE Wireless Communications*, vol. 14, no. 3, pp. 32–43, June 2007.

[3] A. van Zelst and T. C. W. Schenk, "Implementation of a MIMO-OFDM-based wireless LAN system," *IEEE Transactions on Signal Processing*, vol. 52, no. 2, pp. 483–494, February 2004.

[4] H. Suzuki, T. V. A. Tran, and I. B. Collings, "Characteristics of MIMO-OFDM channels in indoor environments," *EURASIP Journal on Wireless Communications and Networking*, vol. 2007, no. 19728, January 2007.

[5] K. Ziri-Castro, W. G. Scalon, and N. E. Evans, "Prediction of variation in MIMO channel capacity for the populated indoor environemnt using a radar cross-section-based pedestrian model," *IEEE Transection on Wireless Communications*, vol. 4, no. 3, pp. 1186–1194, May 2005.

[6] J. D. Gupta, K. Ziri-Castro, and H. Suzuki, "Correlation analysis on MIMO-OFDM channels in populated time varying indoor environment," *10th Australian Symposium on Antennas*, Feb 2007.

[7] J. D. Gupta, K. Ziri-Castro, and H. Suzuki, "Capacity analysis of MIMO-OFDM broadband channels in populated indoor environments," *7th International Symposium on Communications and Information Technologies*, pp. 273–278, Oct 2007.

[8] J. D. Gupta, K. Ziri-Castro, and H. Suzuki, "Dynamic range analysis on MIMO-OFDM broadband channels in a populated time-varying indoor environment," *2007 Australian Telecommunication Networks and Applications Conference*, Dec 2007.

[9] H. Suzuki and A. S. Mohan, "Measurement and prediction of high spatial resolution indoor radio channel characteristic map," *IEEE Transactions on Vehicular Technology*, vol. 49, no. 4, pp. 1321–1333, July 2000.

[10] K. Yu, M. Bengtsson, B. Ottersten, D. McNamara, P. Karlsson, and M. Beach, "Modeling of wide-band MIMO radio channels based on NLoS indoor measurements," *IEEE Transactions on Vehicular Technology*, vol. 53, no. 3, pp. 655–665, May 2004.

[11] H. Suzuki, T. V. A. Tran, I. B. Collings, G. Daniels, and M. Hedley, "Transmitter noise effect on the performance of a MIMO-OFDM hardware implementation achieving improved coverage," *IEEE Journal on Selected Areas in Communications*, vol. 26, no. 6, pp. 867–876, August 2008.

[12] 802.11 Working Group of the 802 Committee, "Draft Standard for Information Technology- Telecommunications and information exchange between systems- Local and metropolitan area networks- Specific requirements- Part 11: Wireless LAN Medium Access Control (MAC) and Physical Layer (PHY) specifications: Amendment 4: Enhancements for Higher Throughput," September 2007.

[13] H. Suzuki, B. Murray, A. Grancea, R. Shaw J. Pathikulangara, and I. B. Collings, "Real-time wideband MIMO demonstrator," *In Proceedings of the 7th International Symposium on Communications and Information Technologies*, pp. 284–289, October 2007.

[14] H. Suzuki, "Accurate and efficient prediction of coverage map in an office environment using frustum ray tracing and in-situ penetration loss measurement," *IEEE Vehicular Technology Conference*, pp. 236–240, April 2003.